

November 1972

LRP 56/72

CENTRE DE RECHERCHES EN PHYSIQUE DES PLASMAS
FINANCÉ PAR LE FONDS NATIONAL SUISSE DE LA RECHERCHE SCIENTIFIQUE

OBSERVATION OF SLOWLY VARYING MAGNETIC INDUCTION
IN A ROTATING MAGNETIC FIELD PINCH

D.W. Ignat, A. Heym, F. Hofmann, and A. Lietti

LAUSANNE

10/11/72

OBSERVATION OF SLOWLY VARYING MAGNETIC INDUCTION
IN A ROTATING MAGNETIC FIELD PINCH

D.W. Ignat, A. Heym, F. Hofmann, and A. Lietti

A b s t r a c t

Recent measurements on a rotating magnetic field pinch reveal in the plasma core large magnetic fields which change slowly in time. Computations based on MHD theory show qualitatively that such fields should be expected, but they fail to reproduce the observed spatial extent and magnitude. Trapping and compression of the induction generated by the first half cycle of the rotating field is apparently a primary cause of the phenomenon.

Introduction

With a rotating magnetic field pinch one attempts to heat and confine a field-free cylindrical plasma column by applying oscillating Z- and θ -pinches dephased by 90° so that the magnetic pressure at the plasma surface is approximately constant in time. Such experiments are motivated by calculations using both collisional (Troyon, 1971) and collisionless (Troyon, 1967; Weibel, 1960) sharp boundary plasma models. These calculations indicate that the surface of a plasma so confined should be stable against all deformations for sufficiently high frequency of field rotation. In addition, qualitative arguments suggest that the magnetic shear associated with diffuse boundaries may enhance stability (Tuck, 1958).

Our laboratory has developed lumped element line generators of large power (≈ 100 MW) and high frequency (2.5 MHz) for driving the θ - and Z-circuits to make such a pinch (Lietti, 1969), and several investigations of this kind of plasma have been reported (Jones et al., 1968; Berney et al., 1971; Berney, 1971).

Recent measurements reveal the existence of large magnetic fields ($\lesssim 1$ kG) inside the plasma which have no frequency components near

the frequency of the applied rf. These fields exist in both θ - and Z-directions and persist in similar form for the filling pressures examined from 10 to 60 mTorr D_2 . Our purpose here is to describe extensive measurements made with a 20 mTorr D_2 initial filling and to present a partial interpretation of the results with the aid of a one dimensional, three fluid MHD simulation of the experiment (Hofmann, 1971a).

Experimental Apparatus

As the apparatus is substantially similar to that reported previously (Berney et al., 1971), we present a brief description emphasizing recent changes. The quartz discharge tube is of 15 cm inside diameter. Ring-shaped molybdenum Z-pinch electrodes fit snugly in the diameter of the tube and are separated by 92 cm, which is 7 cm longer than the length of the θ -pinch compression coil. Return Z-current flows through copper rods imbedded in grooves in the compression coil with epoxy potting. Both lumped element line generators are well matched to the discharge whenever the plasma behaves as a perfectly conducting cylindrical shell of 14 cm diameter.

21

Two unidirectional parabolically shaped Z-current pulses of 22 kA peak current and lasting 5 μ s with a 5 μ s separation preionize the plasma. Immediately afterward fields of the rotating pinch commence with the B_z field (i.e. a θ -pinch) rising first. Twelve periods of generally increasing field are obtained over 5 μ s.

The currents flowing in the Z- and θ -circuits, and thus the B-fields applied to the plasma, are measured with inductive loops. Passive integration ($RC \doteq 10 \mu$ s) of the loop output precedes display on an oscilloscope. Figure 1 shows the applied field obtained with a 20 mTorr D_2 filling and a 28 kV initial charging of the line generator capacitors.

A Mach-Zehnder interferometer yields temporally and radially resolved electron density data by integrating along the plasma axis. The apparatus, working with the $6328 \overset{\circ}{\text{A}}$ line of a He-Ne laser, employs a system of two photomultipliers which permits one to follow the sense of the density variations unambiguously (Heym, 1968). Sensitivity of about 0.01 fringe is achieved corresponding to a minimum measurable density of $5 \times 10^{13} \text{ cm}^{-3}$.

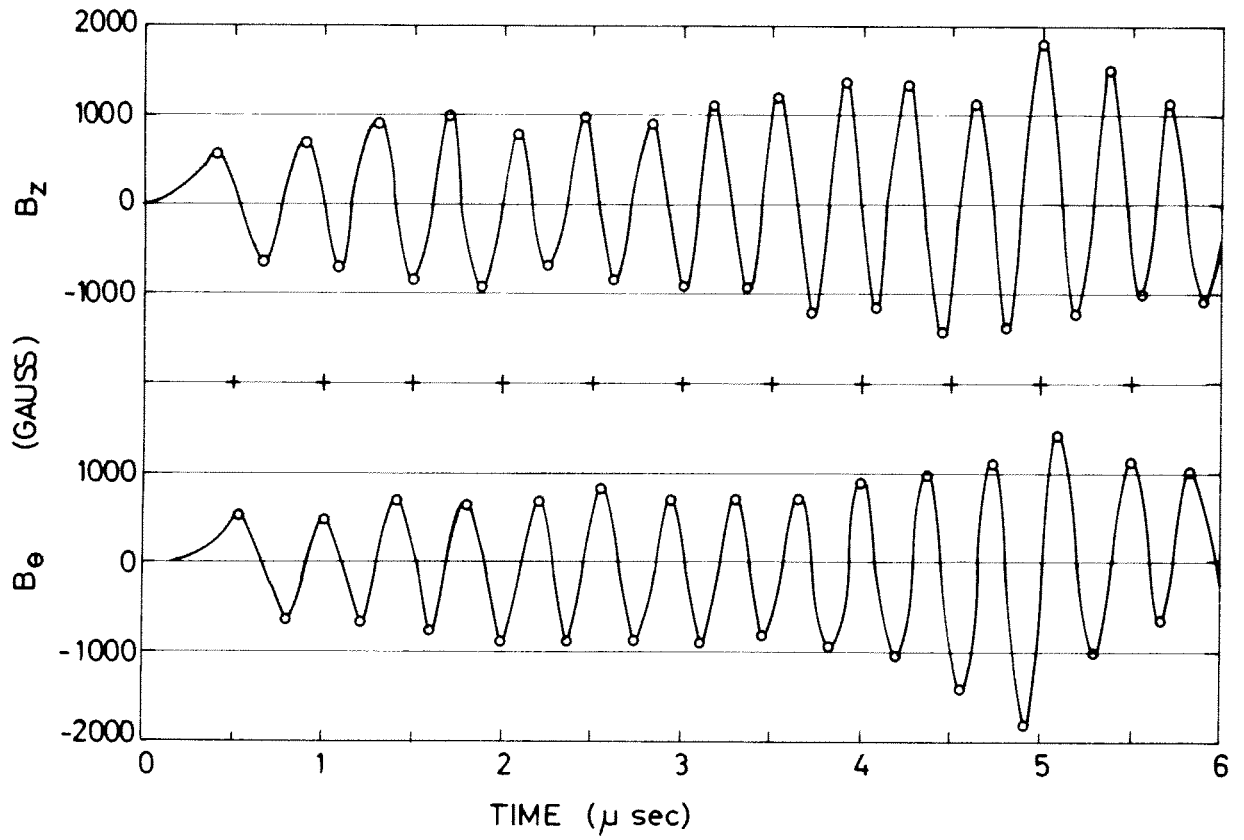


Fig. 1 Measured fields applied to the plasma. B_z and B_θ are dephased by 90° so the field rotates on the plasma surface.

A small double magnetic probe, consisting of two nested coils wound with fine wire and sheathed in quartz allows the simultaneous measurement of both B_{θ} and B_z (Jones et al., 1969) . After passing a differential amplifier, the integrated ($RC \doteq 80 \mu s$) probe signals are completely free of electrostatic pickup (Ignat and Heym, 1972). The system bandwidth is 3 kHz to 6.5 MHz.

Since the probe enters the tube from one end and its carriage mechanism would block the interferometer beam, interior magnetic field measurements and electron density determinations cannot be made at the same time. Measurements reported here come from averages of five shots taken for a given radial position, which is always in the same half diameter in the plane perpendicular to the θ -pinch feed slot. We gather magnetic field data only in the axial mid-plane.

Measurements

Figure 2 depicts in $0.5 \mu s$ intervals the evolution of the electron density $n_e(r)$. Electrodes obstruct measurements within 1 cm of the discharge tube wall. These data indicate

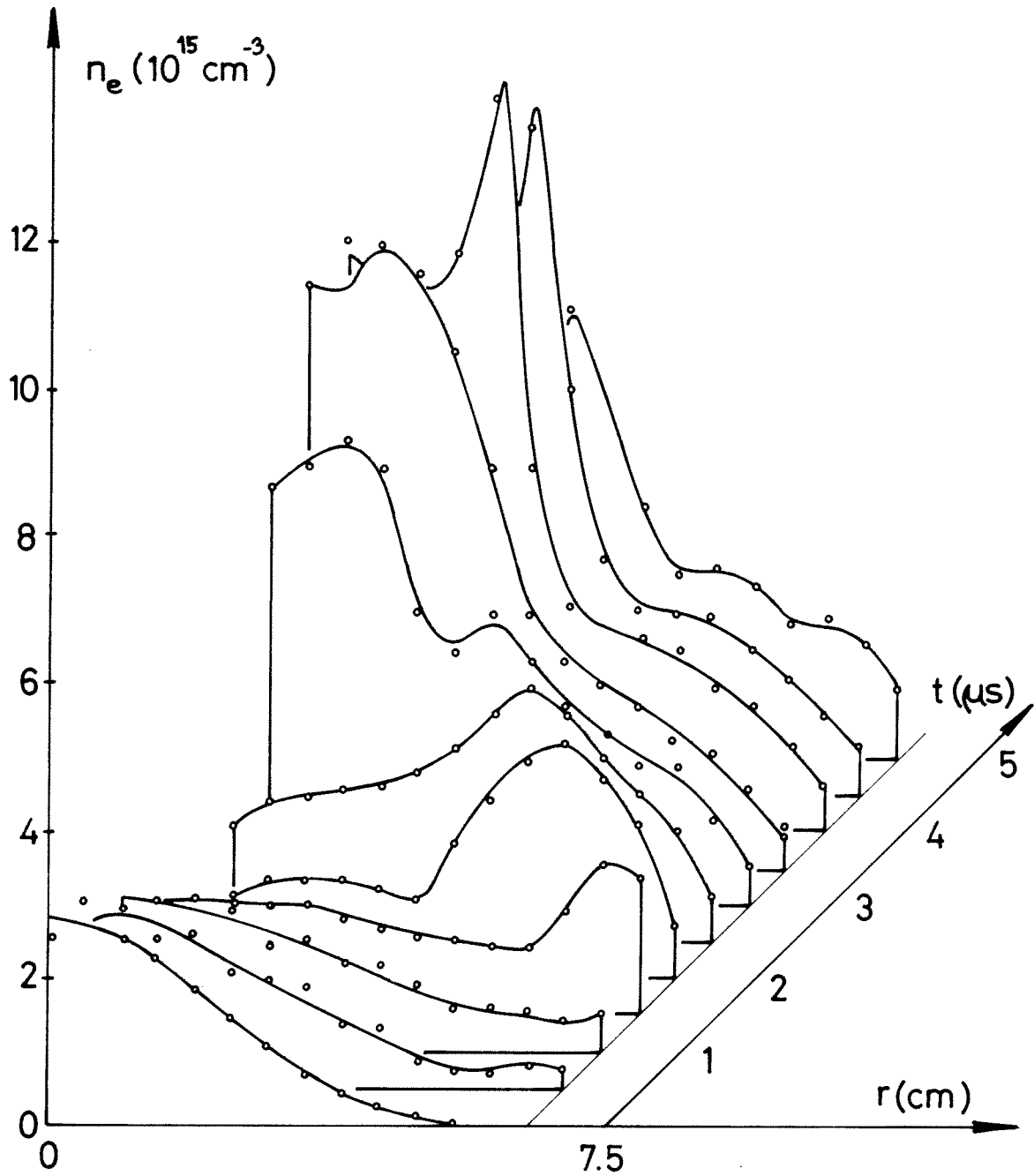


Fig. 2 The time development of the measured electron density as a function of radius.

that peak central plasma density occurs at approximately 3.5 μ s.

The percentage of ionization progresses as in Fig. 3. We define this quantity as the number of electrons measured in the tube divided by the number of D atoms placed there at initial filling. Saturation well above 100 % implies a source of ionizable material at the tube wall.

Interior magnetic fields develop as in Fig. 4. Each curve plots vertically $B_{\theta,Z}(r)$ against radius at the time when the respective field is an extremum at the wall. The relative displacement to later time of the B_{θ} series reflects the 90° phase lag necessary to apply a rotating field at the plasma surface. In each series successive curves represent time changes of about 0.2 μ s, the rf half-period. The wide swings about zero caused by the rf nature of the applied field confuse the right side of each graph. Between $r = 0$ and $r = 6$ cm one clearly sees the development of fields which do not change sign in time but which grow to over 1 kG on the axis in the Z-component. These data are averaged from five shots each taken at 16 different radial positions ($r = 0, 2.5, 4, 5, 5.5, 6, 6.3, 6.5, 6.7, 6.9, 7, 7.1, 7.2, 7.3, 7.4, 7.5$ cm).

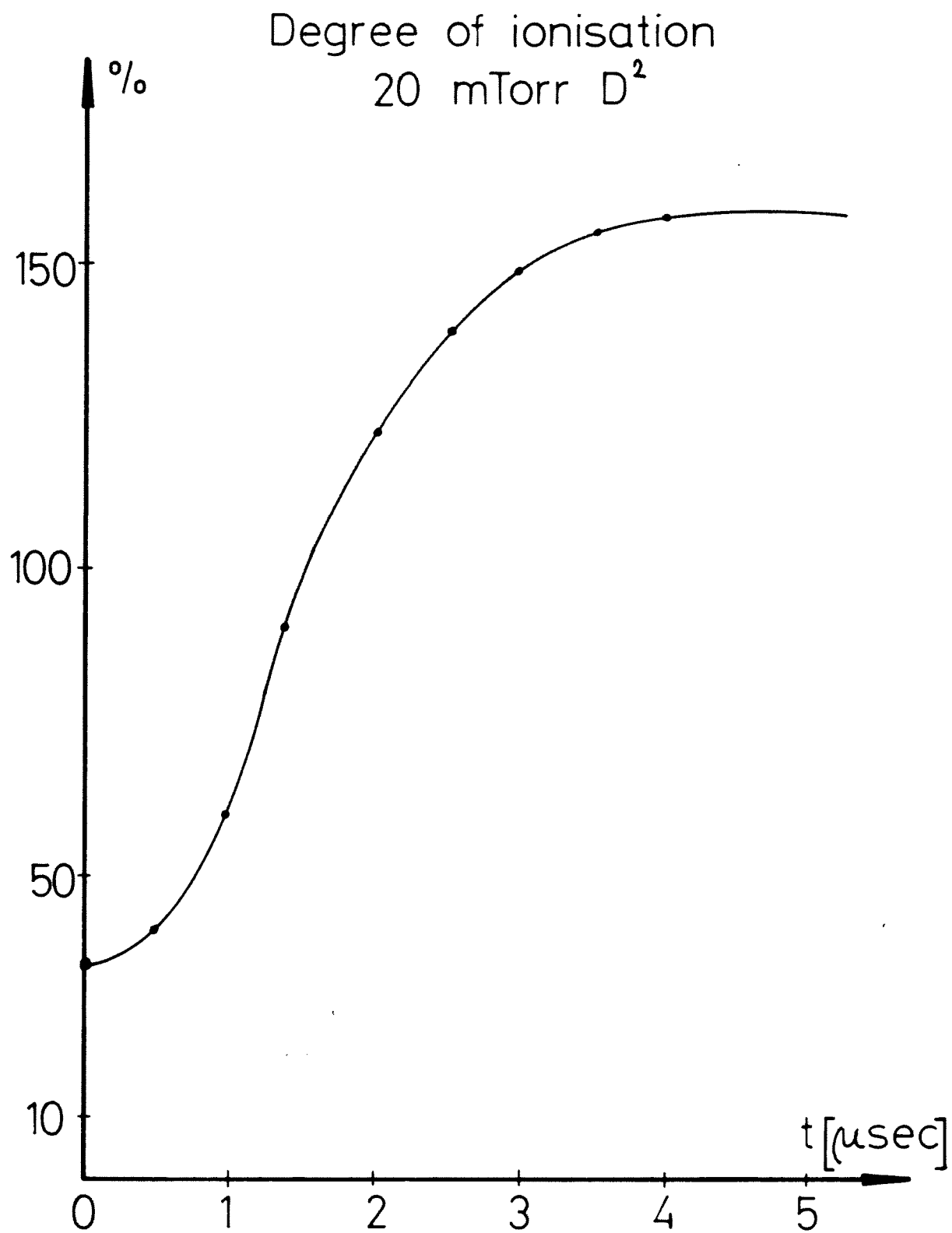


Fig. 3 The ratio of the number of electrons measured in the tube to the number placed there in initial filling.

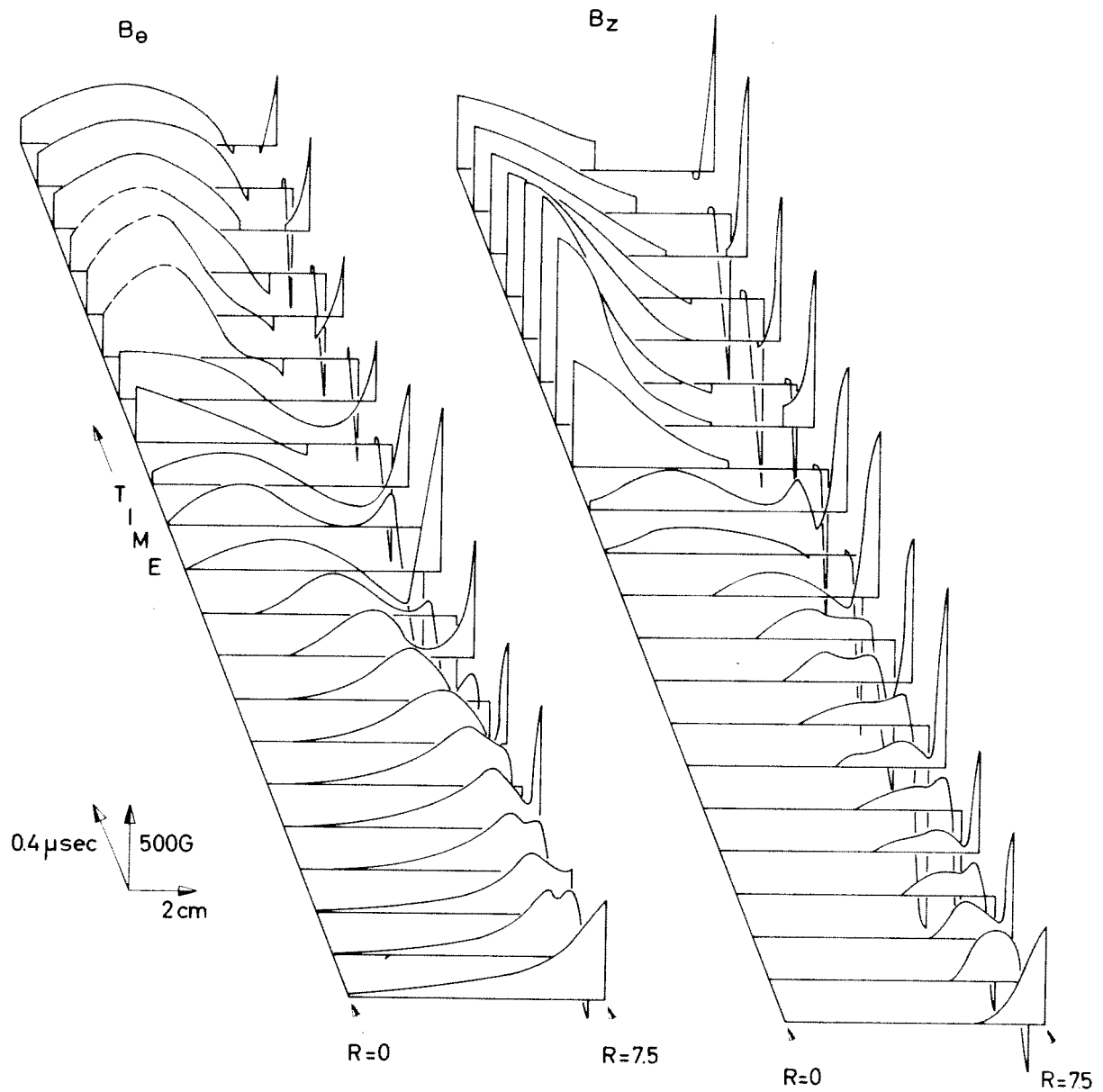


Fig. 4 The time development of $B_\theta(r)$ and $B_z(r)$ as determined from magnetic probes.

For clarity no attempt is made here to indicate the degree of scatter, which changes considerably with both radius and time. Generally, scatter is small (1) at early times, (2) near the center, and (3) very near the wall. Where shot-to-shot variation is so large that one does not know where to draw the curve, only the abscissa remains. (See intermediate radii at large times). The dashed lines indicate that measured points are too distant to permit confident interpolation between observations.

The first B_{θ} curve shows field extending to small radii. Circulating Z-currents excited by the two unidirectional preionization (PI) pulses account for most of this interior field. We observed in a brief trial, without the support of the large amount of data given here, that changing the direction of the PI current does not alter the sense of the large quasi-dc fields observed in the experiment.

Cylindrical symmetry dictates $B_{\theta}(r = 0) = 0$, but we always measure some B_{θ} on axis. The sense, however, appears to be random. In our five shots, three had the sense shown, and we averaged only those three to save the impression that strict symmetry is not observed. Some trial measurements revealed the

existence of B_r also, confirming the lack of symmetry.

The cross-plotted experimental data suggest to us the following simple physical interpretation of the measurement. The first half cycle of the applied field penetrates deeply the cold pre-ionized plasma. Soon thereafter large diamagnetic currents heat the plasma skin and drop its resistivity, and thus interior field is trapped. Plasma compression proceeds due to a combination of magnetic compression, pressure exerted by the hot plasma at the wall, and inertial effects. This collapse multiplies the trapped field faster than resistivity can diffuse it, yielding our observed effect. In addition, the B_θ field imparted by the preionization at $t = 0$ also may contribute to the large B_θ fields we measure. Simple quantitative explanations of observations are difficult to construct because of the complexity of the process involved.

MHD Simulations

As the existence of large dc magnetic fields in the plasma is both unexpected and intriguing, we pursued MHD simulations of the experiment to discover how well this phenomenon can be

quantitatively understood. Comparative studies of the measured and calculated electron densities and rf field penetration (see Hofmann, 1971b) were not made in the present work.

Initial conditions used in the MHD code (Hofmann, 1971a) were (1) $n_e(r, t = 0)$ as measured interferometrically, (2) assumed electron, ion, and neutral temperatures of 1 eV, (3) radially constant neutral density consistent with the 20 mTorr D_2 filling and the measured initial number of electrons. In some cases the initial $B_\theta(r)$ left by the PI was also included. For boundary conditions on the field we insert the applied $B_{\theta, Z}(t)$ as measured using the exterior current probe.

The code permitted variation of a large number of physical and computational parameters. Numerical experimentation disclosed that large anomalous resistivity was essential to reproduce the measurements even approximately.

We introduce anomalous resistivity ($\eta_{\text{anom.}}$) to the computation in the following ad hoc manner. Since large streaming velocities exist we assume η_{anom} is proportional (through the parameter α) to the semi-empirical resistivity given by Buneman after exami-

nation of the non-linear development of the electron-ion two-stream instability (Buneman , 1959). To include an electric field dependence in η_{anom} we multiply by the ratio of electron drift speed (V_D) to electron thermal speed (V_{Te}) raised to the first power and the unit step function of $V_D - V_{Ti}$.

$$\eta_{anom} = \alpha (200 \pi \epsilon_o \omega_{pe})^{-1} \cdot (V_D/V_{Te}) \cdot U(V_D - V_{Ti})$$

In terms of an effective anomalous collision frequency ν_{eff} this assumption takes the form

$$\nu_{eff} = \alpha \frac{0.3}{\pi} \omega_{pi} \cdot (V_D/V_{Te}) \cdot U(V_D - V_{Ti})$$

The total resistivity is the sum of the anomalous term and the classical result (Spitzer resistivity plus that from electron-neutral collisions).

By varying α holding all other parameters constant, we sought the best fit for $B_z(r = 0, t)$ since this quantity disclosed the most spectacular and reproducible behavior in the experiment. Figure 5 exhibits averaged measurements with typical error bars (bar length is 2 x RMS deviation

from average) and computed curves for three α values.

The best fit occurs for $\alpha = 1$. In analyzing other measurements on a similar experiment with the same code, Hofmann found data most successfully reproduced computationally for α 's between 0.3 and 3.0 (Hofmann, 1971b).

Now taking $\alpha = 1$, we examine in Fig. 6 the comparison for $B_{\theta, Z}$ at $r = 2.5$, and 4.0 , positions where dc fields are large and reproducibility acceptable. The agreement here is only qualitative. Computation yields dc fields of the proper sense, but magnitudes are too small and the details of time behavior are dissimilar.

We experimented with inclusion of $B_{\theta}(r, t = 0)$ in initial conditions of the computation and found minute influence on $B_Z(r, t)$. This inclusion can boost or diminish dc levels of $B_{\theta}(r, t)$ for early times, but it has little effect on the behavior after $3 \mu s$. Figure 7 presents measured $B_{\theta}(t)$ at $r = 2.5, 4$ and computed curves ($\alpha = 1$). The computation assumes both the actual sense of $B_{\theta}(t = 0)$ (solid line) and the opposite sense (dashed line). The simple analytic form employed in fitting data causes the small variance at $t = 0$.

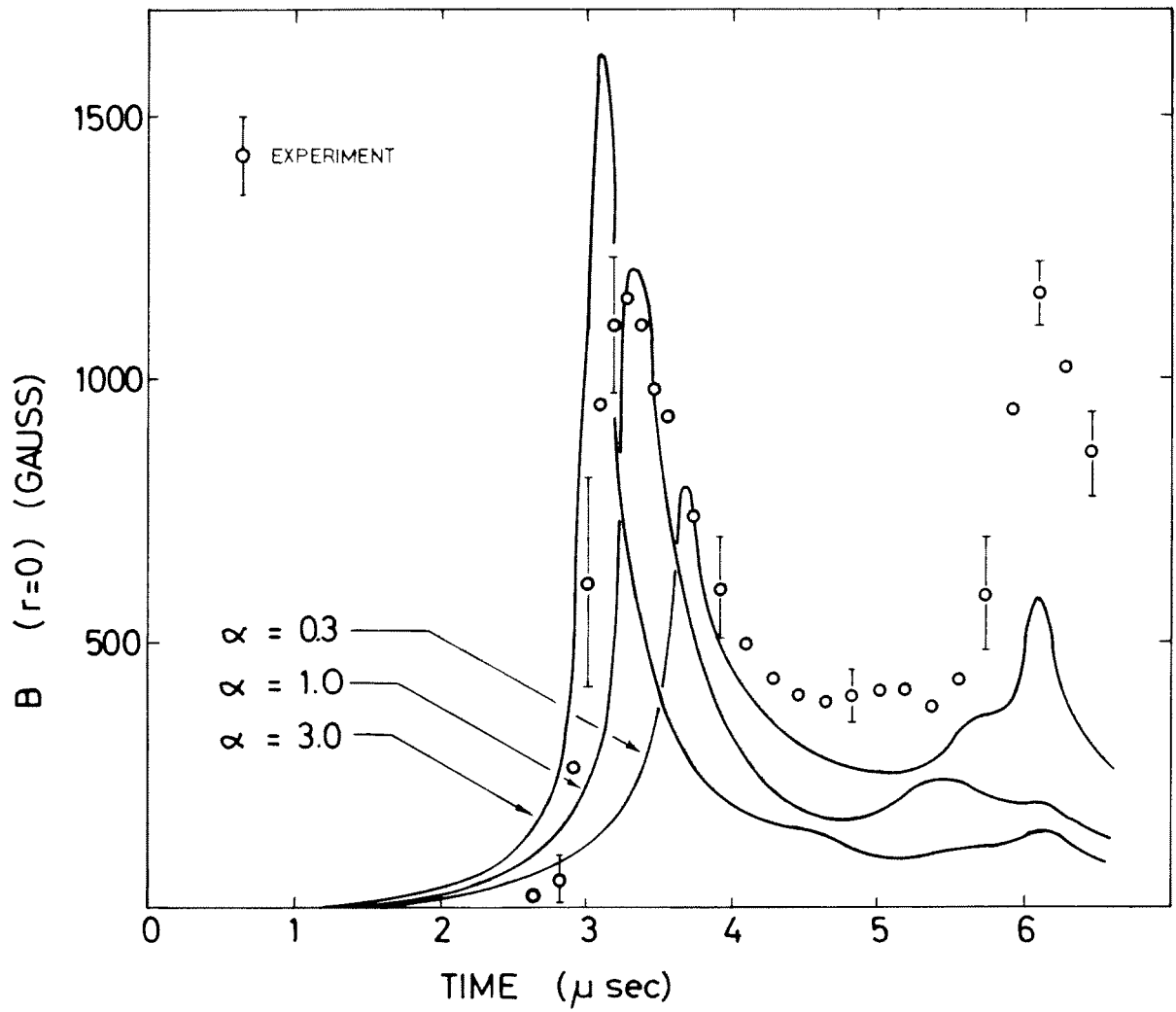


Fig. 5 Measured behavior of $B_z(r=0)$ and MHD prediction for various anomalous resistivity parameter values.

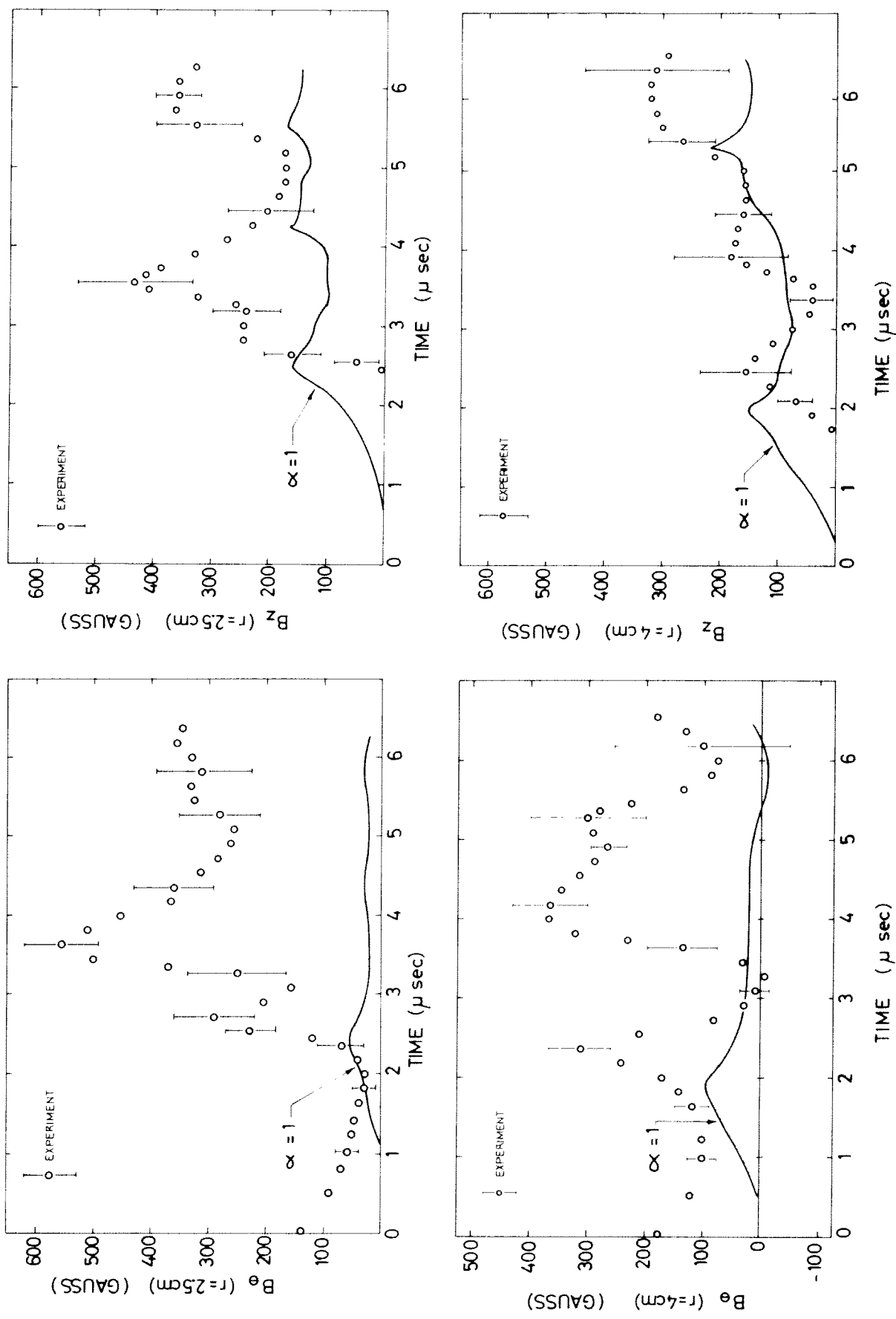


Fig. 6 Measured field behavior compared with MHD code results at $r = 2.5$ cm and 4.0 cm,

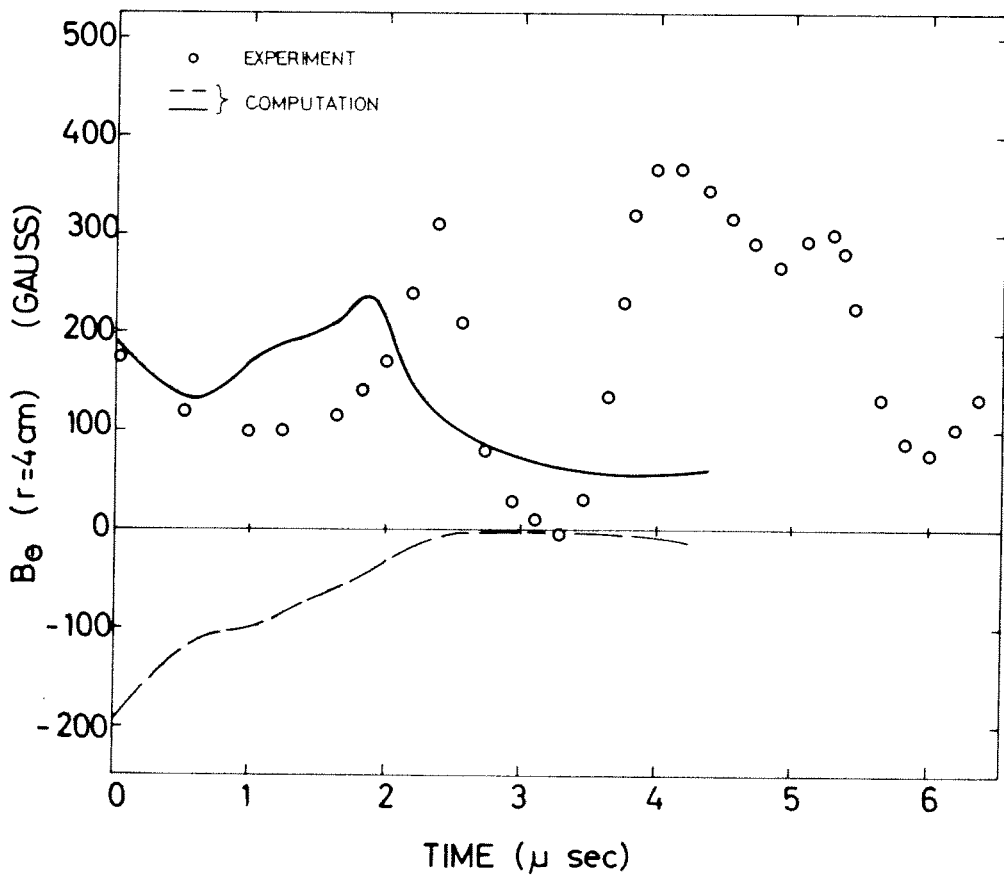
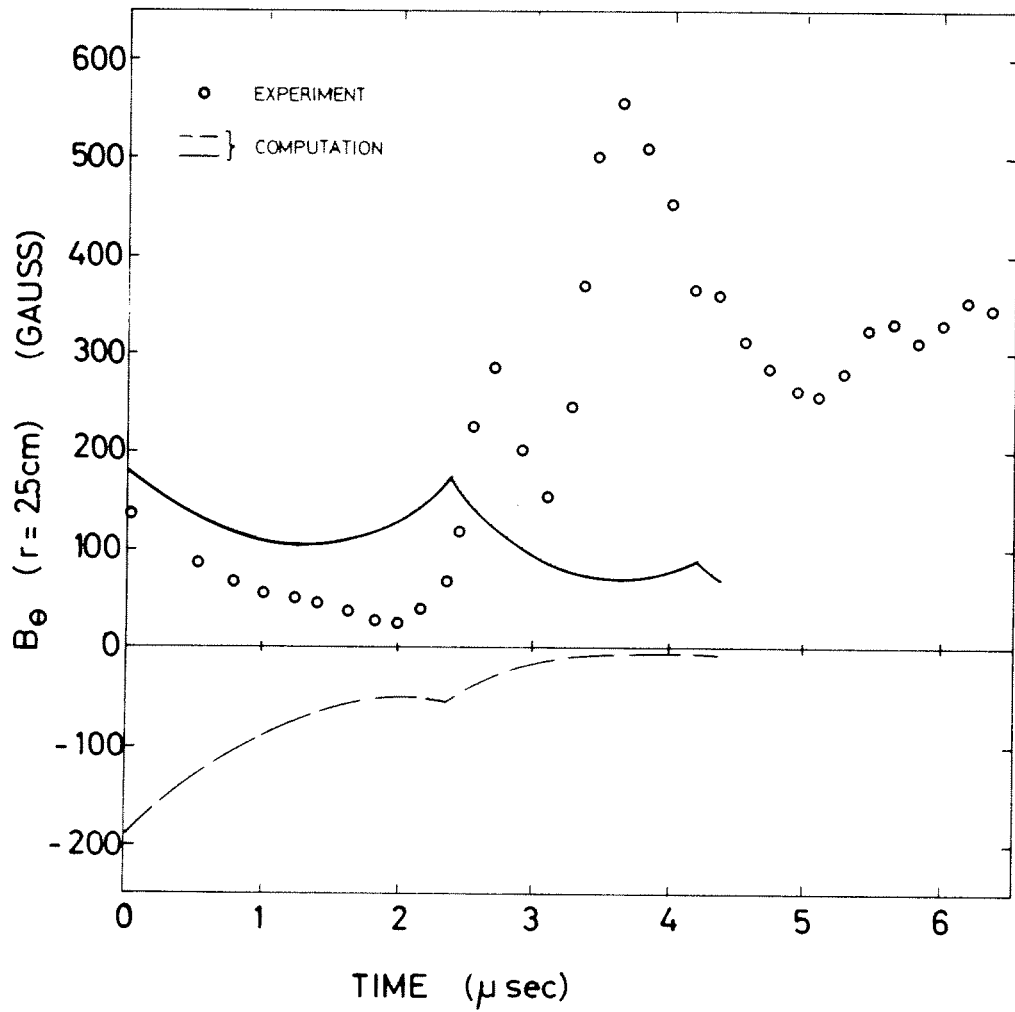


Fig. 7 Experimental data compared with computations which use a fit to the measured field remaining from pre-ionization in initial conditions.

Figure 8 depicts the computed evolution of $B_{\theta,Z}(r)$ if $B_{\theta}(r, t = 0) = 0$. Plotting scales and conventions are the same as in Fig. 4 where measurements are graphed. Similar is Fig. 9, but the PI-stimulated $B_{\theta}(t = 0)$ is also an initial condition. The general qualitative agreement between the measurements and the calculations is unmistakable in these plots. However, careful examination reveals the same important shortcomings in the agreement that are very evident in Figs. 6 and 7. That is, the computed dc components of B_Z are large only near the center and computed dc components of B_{θ} do not reach the 500 Gauss levels which are measured. Figures 10a and 10b show the computed $n_e(r)$ evolution corresponding to the Figs. 8 and 9 respectively. These graphs are plotted similarly to the density measurements.

We are not able to improve the experiment-theory correspondence shown in Figs. 5-7 by any of the following means: (1) inclusion of axial heat conductivity, (2) postulation of anisotropic resistivity and thermal conductivity, (3) further adjustment of α , and (4) assumption of anomalous resistivity which varies with V_D/V_{Te} as a smoothed step function.

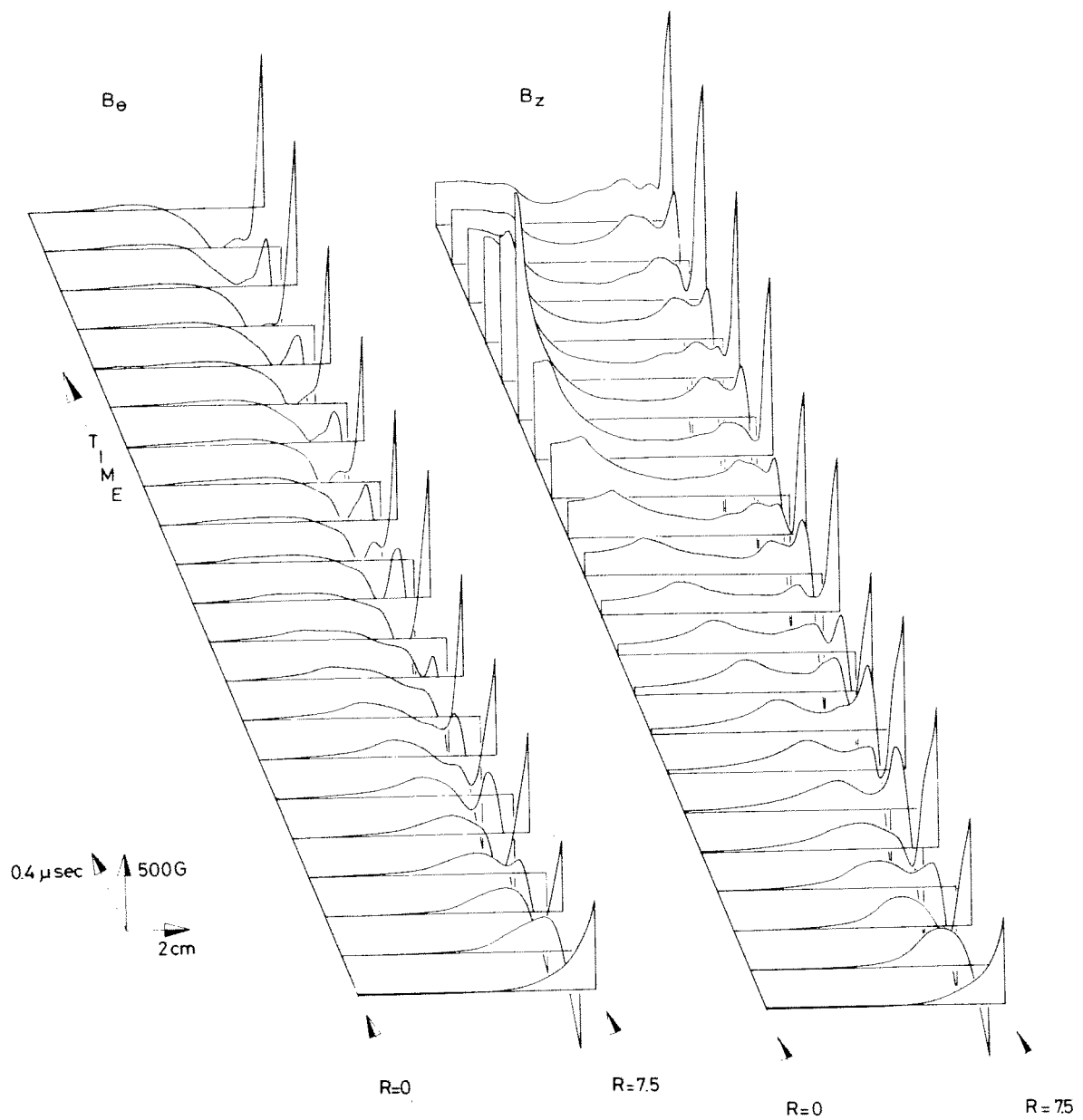


Fig. 8 Computed evolution of the interior magnetic field
 assuming $\alpha = 1$.

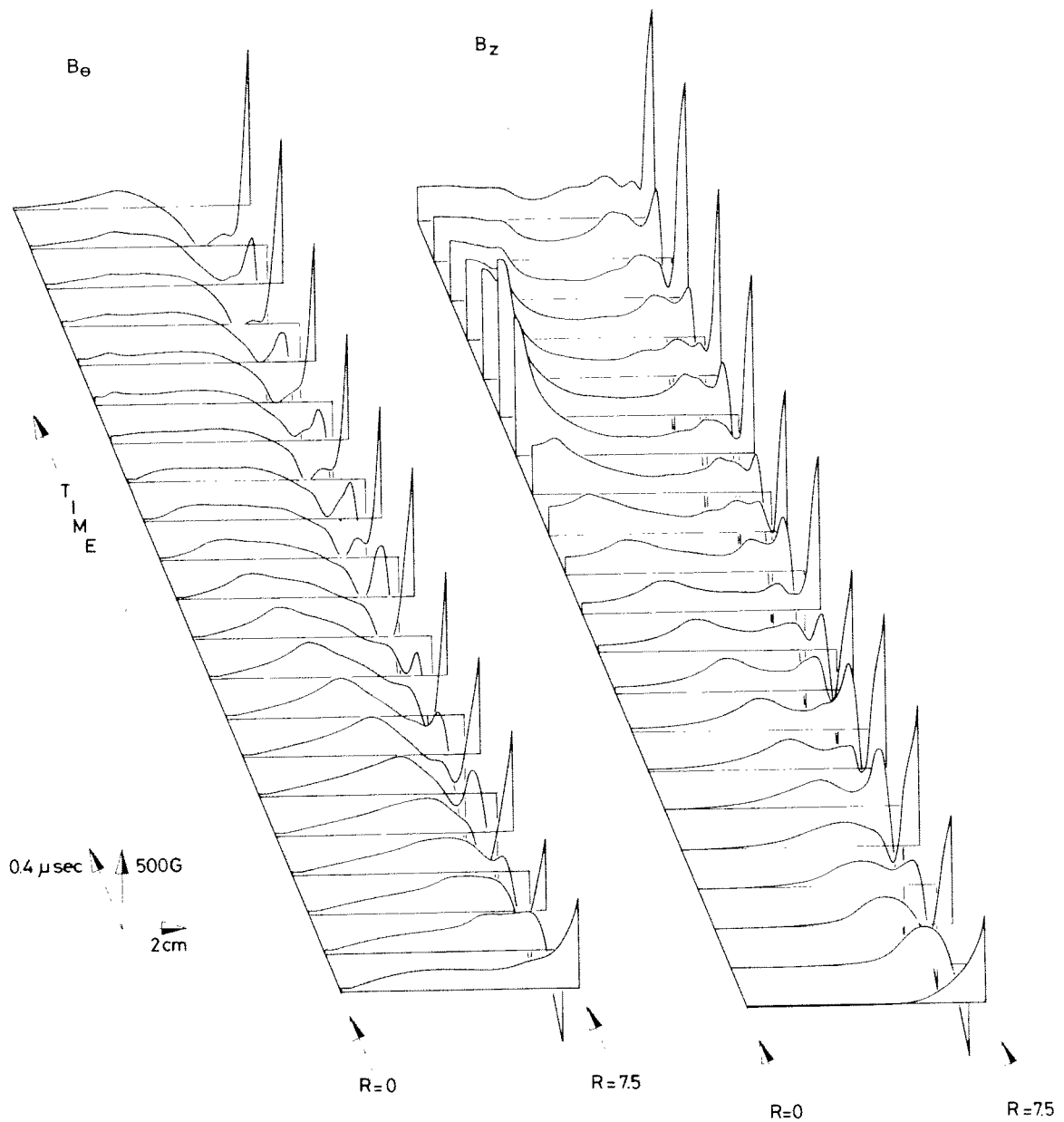


Fig. 9 Computed evolution of the interior magnetic field assuming $\alpha = 1$ and using the initial B_θ excited by the preionization in initial conditions.

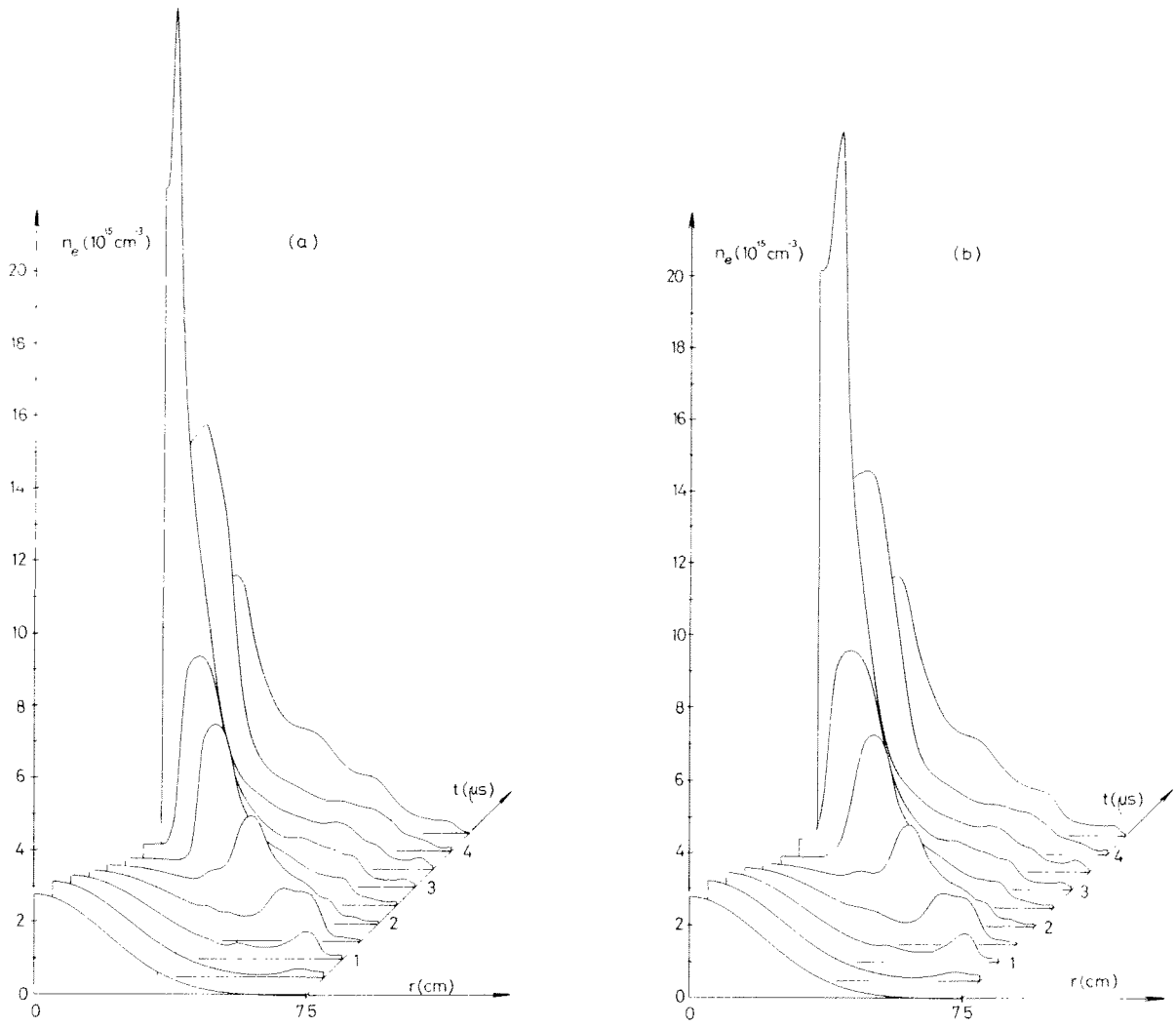


Fig. 10 Computed electron density evolution assuming $\alpha = 1$ both not using (a) and using (b) $B_{\theta}(r, t=0)$ in initial conditions.

There are some other possibilities for improving the agreement which we did not try. We did not change the mesh size (now 40 cells in the radius), nor did we study the effects of postulating various magnitudes and time dependences of material flux from the discharge tube wall.

Conclusion

We have shown experimentally that plasma suddenly irradiated by a rf magnetic field can develop spontaneously large dc fields in the plasma core. We believe that the basic mechanism for this process is the trapping and compression of flux from the first rf period. Simulation of the experiment using one dimensional fluid equations confirms our observations although not with great quantitative accuracy. We feel that the moderate success of the computation is acceptable under the circumstances.

Acknowledgements

We are indebted to P. Hafner for the preionization circuit, H. Ripper for the magnetic probes and vacuum maintenance, and E. Burki, C. Corboz, E. Striberni and G. Ziegenhagen for general assistance with the experiment. This work was supported by the Fonds National Suisse de la Recherche Scientifique.

References

- BERNEY A. (1971) Helvetica Physica Acta 44, 213.
- BERNEY A., HEYM A., HOFMANN F. and JONES I.R. (1971)
Plasma Physics 13, 611.
- BUNEMAN O. (1959) Phys. Rev. 115, 503.
- HEYM A. (1968) Plasma Physics 10, 1069.
- HOFMANN F. (1971a) Report LRP 46/71, this Laboratory.
- HOFMANN F. (1971b) in Plasma Physics and Controlled Nuclear
Fusion Research, IAEA, Vienna, Volume I, p. 267.
- IGNAT D.W. and HEYM A. (1972) Report 55/72, this
Laboratory. Submitted for publication.
- JONES I.R., LIETTI A. and PEIRY J.-M. (1968)
Plasma Physics 10, 213.
- JONES I.R., PEIRY J.-M. and COCQ D. (1969)
Rev. Sci. Inst. 40, 133.
- LIETTI A. (1969) Rev. Sci. Inst. 40, 473.
- TROYON F. (1967) Phys. Fluids 10, 2660.
- TROYON F. (1971) Plasma Physics 13, 715.
- TUCK J.L. (1958) in Second United Nations Int. Conf. on the
Peaceful Uses of Atomic Energy, Geneva,
Volume 32, p. 3. United Nations.
- WEIBEL E.S. (1960) Phys. Fluids 3, 946.